FULL PAPER

BJC

British Journal of Cancer (2014) 110, 304–312 | doi: 10.1038/bjc.2013.738

Keywords: gemcitabine; pharmacogenomics; population pharmacokinetic model; covariates; dFdCTP; infusion rate

SLC28A3 genotype and gemcitabine rate of infusion affect dFdCTP metabolite disposition in patients with solid tumours

A Khatri[1], B W Williams[1,2], J Fisher[1,2], R C Brundage[1], V J Gurvich[3,4,5], L G Lis[4], K M Skubitz[5,6], A Z Dudek[5,6], E W Greeno[5,6], R A Kratzke[5,6], J K Lamba[1,5,7] and M N Kirstein*[,1,2,5,7]

[1]*Department of Experimental and Clinical Pharmacology, College of Pharmacy, University of Minnesota, Minneapolis, MN 55414, USA;* [2]*Clinical Pharmacology Shared Resource of Masonic Comprehensive Cancer Center, University of Minnesota, Minneapolis, MN 55414, USA;* [3]*Department of Medicinal Chemistry, College of Pharmacy, University of Minnesota, Minneapolis, MN 55414, USA;* [4]*Institute for Therapeutics Discovery and Development, College of Pharmacy, University of Minnesota, Minneapolis, MN 55414, USA;* [5]*Masonic Comprehensive Cancer Center, University of Minnesota, Minneapolis, MN 55455, USA;* [6]*Department of Medicine, School of Medicine, University of Minnesota, Minneapolis, MN 55455, USA and* [7]*PUMA-Institute of Personalized Medicine, College of Pharmacy, University of Minnesota, Minneapolis, MN 55455, USA*

Background: Gemcitabine is used for the treatment of several solid tumours and exhibits high inter-individual pharmacokinetic variability. In this study, we explore possible predictive covariates on drug and metabolite disposition.

Methods: Forty patients were enrolled. Gemcitabine and dFdU concentrations in the plasma and dFdCTP concentrations in peripheral blood mononuclear cell were measured to 72 h post infusion, and pharmacokinetic parameters were estimated by nonlinear mixed-effects modelling. Patient-specific covariates were tested in model development.

Results: The pharmacokinetics of gemcitabine was best described by a two-compartment model with body surface area, age and NT5C2 genotype as significant covariates. The pharmacokinetics of dFdU and dFdCTP were adequately described by three-compartment models. Creatinine clearance and cytidine deaminase genotype were significant covariates for dFdU pharmacokinetics. Rate of infusion of $<25\,mg\,m^{-2}\,min^{-1}$ and the presence of homozygous major allele for SLC28A3 (CC genotype) were each associated with an almost two-fold increase in the formation clearance of dFdCTP.

Conclusion: Prolonged dFdCTP systemic exposures ($\geqslant$72 h) were commonly observed. Infusion rate $<25\,mg\,m^{-2}\,min^{-1}$ and carriers for SLC28A3 variant were each associated with about two-fold higher dFdCTP formation clearance. The impacts of these covariates on treatment-related toxicity in more selected patient populations (that is, first-line treatment, single disease state and so on) are not yet clear.

Gemcitabine (2′,2′-difluorodeoxycytidine, dFdC), a pyrimidine antimetabolite, has broad-spectrum activity against several solid tumours and is approved for treatment of pancreatic, breast, ovarian and non-small cell lung cancers. After administration, gemcitabine is metabolised primarily by the plasma and liver cytidine deaminase to 2′,2′-difluorodeoxyuridine (dFdU), which has little antitumour activity. Gemcitabine is transported into cells and undergoes intracellular phosphorylation by deoxycytidine kinase (DCK) to its monophosphate metabolite (dFdCMP), which subsequently gets metabolised by nucleotide kinases to its active diphosphate (dFdCDP) and triphosphate (dFdCTP) metabolite (Wong *et al*, 2009). The cytotoxic effect of gemcitabine is attributed mainly to the combined effects of the di- and tri-phosphate nucleosides, which leads to inhibition of DNA synthesis

*Correspondence: Dr MN Kirstein; E-mail: kirst002@umn.edu

Received 9 August 2013; revised 15 September 2013; accepted 23 October 2013; published online 3 December 2013

(Wong *et al*, 2009). Although much less potent than dFdCTP, dFdU is also formed intracellularly and can be phosphorylated to form triphosphate molecules with radiosensitising, cytotoxic and hepatotoxic effects (Pauwels *et al*, 2006; Veltkamp *et al*, 2008; Benyumov *et al*, 2011).

There are numerous reports on the pharmacokinetics of gemcitabine and dFdU in patients; however, only a few clinical studies have described the pharmacokinetics of the active metabolite, dFdCTP. A mass-balance study reported that a median of 77% (range: 30–96%) of the administered dose of gemcitabine was excreted within 24 h in urine, of which a median of 5% was excreted as unchanged gemcitabine (Abbruzzese *et al*, 1991). The pharmacokinetics of dFdCTP has been evaluated in circulating leukaemic cells or peripheral blood mononuclear cells (PBMCs) as a surrogate for tumour (Grunewald, 1990; Tempero *et al*, 2003; Tham *et al*, 2008).

Saturable formation of dFdCTP from gemcitabine has been postulated. *In vitro* incubation of leukaemia cells for 1 h with gemcitabine concentrations ranging from 2.5 to 100 μM resulted in maximum cellular accumulation of dFdCTP at 15–20 μM gemcitabine (Grunewald *et al*, 1990). In another study, investigators incubated PBMCs *in vitro* with gemcitabine concentrations ranging from 2.5 to 100 μM for 2 h and found that the accumulation of dFdCTP was maximal at 10–15 μM gemcitabine (Grunewald *et al*, 1991). In a phase 1 dose-ranging study testing gemcitabine doses ranging from 53 to 1000 mg m^{-2}, the rate of dFdCTP accumulation and C_{max} were highest following a dose of 350 mg m^{-2} over 30 min at which steady-state plasma concentrations of gemcitabine ranged from 15 to 20 μM (Grunewald *et al*, 1991). Another phase 1 study, evaluating gemcitabine doses ranging from 10 to 1000 mg m^{-2} over 30 min, showed that peak dFdCTP concentration in PBMCs did not increase following gemcitabine doses higher than 350 mg m^{-2} (Abbruzzese *et al*, 1991). On the basis of these results, others have investigated prolonged gemcitabine infusions to keep the plasma gemcitabine concentrations within 15–20 μM to maximise the accumulation of dFdCTP. A population pharmacokinetic analysis reported that saturable formation of dFdCTP does not occur at 1000 mg m^{-2} dose of gemcitabine when administered over 30 min (Tham *et al*, 2008). Hence, there is evidence both in support as well as against the saturable formation of dFdCTP from gemcitabine. As dFdCTP is one of the major active metabolites, a better understanding of its pharmacokinetics is the first step towards understanding possible association between inter-patient pharmacokinetic variability and treatment outcomes. The primary objectives of this study were (i) to estimate inter-patient gemcitabine and metabolite pharmacokinetic variability and associations with patient-specific covariates (for example, genotype) and (ii) to investigate the possible impact of gemcitabine infusion rate on the disposition of the active metabolite, dFdCTP. Such information could eventually be helpful in dose optimisation of gemcitabine.

MATERIALS AND METHODS

Patients. Adult patients ($\geqslant$18 years old) diagnosed with solid tumours for which treatment with intravenous gemcitabine, either as single agent or in combination with other chemotherapeutic drugs, was already planned by clinicians were enrolled in the study. The study protocol was approved by the University of Minnesota institutional review board and a signed informed consent from all patients was obtained before participation in the study. The following information was prospectively collected from each patient: age, height, weight, body surface area (BSA), gender, smoking status, liver function tests (AST, ALT) and serum creatinine.

Pharmacokinetic study. A total of 40 patients were enrolled in the study. Blood samples were obtained at the following times: pre-infusion, 5, 15, 30, 45 min, and 1, 1.25, 1.5, 2, 6, 24, 48 and 72 h after the end of gemcitabine infusion. Six and 72 h post-infusion sampling times were optional. At each sampling time, 8 ml of blood was drawn into Ficoll-Hypaque tubes (BD Vacutainer CPT; Becton, Dickinson and Company, Franklin Lakes, NJ, USA) pre-loaded with 10 mg ml^{-1} concentration of tetrahydrouridine (1 : 125 :: tetrahydrouridine : blood) to prevent *ex vivo* metabolism of gemcitabine to dFdU. Immediately after separating plasma by centrifugation, the PBMCs were isolated as per manufacturer's procedure. Plasma samples were stored at $-80\,^{\circ}$C until analysis. The number of PBMCs in blood at each sampling time was determined using haemocytometer. Peripheral blood mononuclear cells were lysed with 0.5 ml of ice-cold methanol: water (70 : 30), and stored at $-80\,^{\circ}$C until analysis.

Analytical methods. Gemcitabine and dFdU concentrations in plasma samples were measured by validated high-performance liquid chromatography (HPLC) assays with UV detection or tandem mass spectrometry (LC-MS/MS) based on a previously published report (Kirstein *et al*, 2006). The lower limit of quantification (LLOQ) of the HPLC-UV assay was 0.01 μM for gemcitabine and 2 μM for dFdU. The LLOQ of the LC-MS/MS assay was 0.05 μM for gemcitabine and 0.08 μM for dFdU. The dFdCTP concentrations were measured in PBMCs by a validated HPLC-UV assay in the majority of the patients and by a more sensitive, validated LC-MS/MS assay in some patients (Veltkamp *et al*, 2006). The LLOQ of the HPLC-UV assay for dFdCTP was 53 pM and that of LC-MS/MS was 1 pM. The concentrations of dFdCTP were corrected for the number of PBMCs in each blood sample and expressed as pM per one million cells. The concentrations of intracellular dFdCTP were corrected for the mean cell volume of PBMCs to convert the units of concentration from mass per million cells to mass per volume (Cheung *et al*, 1982). By doing so, dFdCTP was assumed to be uniformly distributed among all of the cells in each sample as done by others (Tham *et al*, 2008). We tested the estimation of separate residual unexplained variance (RUV) parameters for the HPLC-UV and LC-MS/MS assays used in the analysis of gemcitabine, dFdU and dFdCTP concentrations to account for the differences in their precision and sensitivity. The separate residual variances (RUV) for the different assays were not significant; hence, only one RUV parameter was estimated in the final model.

Synthesis of *tris*(triethylammonium) salt of dFdCTP. Tris(triethylammonium) salt of dFdCTP was synthesised for preparing the standard curve for dFdCTP assay. The synthetic approach used in this work was largely based on the methodology pioneered by Bogachev (1996) for trisodium salts and applied by Risbood *et al* (2008) for the synthesis of triethylammounium salts of dFdCTP. The Bogachev two-step approach is the only synthetic strategy for dFdCTP reported to date. Most recently, a three-step microbiological approach to the synthesis of this compound has been published (Lohman and Stubbe, 2010). In our work, a modified purification procedure that allowed to improve the purity and increase yields of both dFdCMP and dFdCTP was developed.

Gemcitabine hydrochloride was phosphorylated with phosphorus oxychloride in trimethylphosphate at 5 °C. However, our attempts to purify the monophosphate dFdCMP using the Risbood methodology have not resulted in satisfactory purity (Risbood *et al*, 2008). Therefore, we purified the monophosphate by flash chromatography on silica gel using a four-component system (dichloromethane-methanol-water-ammonium hydroxide, 5 : 3 : 0.5 : 0.05) as eluent. Then the monophosphate dFdCMP was converted into the triphosphate dFdCTP by treatment with trifluoroacetic anhydride in the presence of triethylamine and *N*,*N*-dimethylaniline in acetonitrile at $-5\,^{\circ}$C. The intermediate

trifluoroacetate was treated with 1-methylimidazole and triethylamine to produce monophosphate *N*-methylimidazolide. The latter was treated with *tris*(tetrabutylammonium) hydrogen pyrophosphate in acetonitrile followed by purification on DEAE Sephadex A25 converted into the OH^- form. In order to achieve a better purification and recovery of the product, the sorbent/substrate ratio was increased by 2.5-fold compared with that previously reported (Risbood *et al*, 2008). The product was then lyophilised. The final *tris*(triethylammonium) salt of dFdCTP was prepared from dFdCMP with the yield of 24 and 95% purity, which represent a moderate improvement in comparison with the previously published procedures (Bogachev, 1996; Risbood *et al*, 2008).

Genotyping. Genomic DNA was isolated from whole blood for genotyping. As described previously, DNA isolation and quantitation from blood samples were performed using QIAamp DNA Blood Midikit (Qiagen Inc., Valencia, CA, USA) and Nanodrop ND-8000 spectrophotometer (Thermo Fisher Scientific, Waltham, MA, USA), respectively. A total of 111 SNPs within nine genes involved in the gemcitabine cellular transport and metabolic pathway such as − CDA, CMPK, DCK, DCTD, NT5C2, NT5C3, SLC28A1, SLC28A3 and SLC29A1 were selected for genotyping using a Sequenom platform that uses MALDI-TOF-based chemistry (Mitra *et al*, 2012). Several selection criteria including, functional importance (for example, coding SNPs, regulatory SNPs and splice site SNPs), literature reports and TagSNPs within the candidate genes identified using data from European ancestry (US residents of northern and western European ancestry (CEU)) HapMap samples and restriction to within 2 kb upstream and downstream of the gene were used to select these 111 SNPs for genotyping.

To reduce the number of SNPs to be evaluated as significant covariates in pharmacokinetic model described in the next section, we first used selection and filtering criteria that include only considering SNPs in the Hardy–Weinberg equilibrium, linkage disequilibrium and with minor allele frequency >0.1 to select 37 SNPs. These 37 SNPs were then analysed for associations with the *post hoc* pharmacokinetic parameters following population pharmacokinetic modelling. We identified seven SNPs residing in six metabolic pathway genes that were significant for either gemcitabine clearance, dFdU clearance or dFdCTP formation clearance (Mitra *et al*, 2012). Those seven SNPs (listed in Table 1) were subsequently tested as covariates in the final population pharmacokinetic model during covariate model building.

Table 1. Patient characteristics

Patient characteristics	Median (range)
Age (years)	64 (20–87)
Sex	22 females, 18 males
Weight (kg)	79 (58–132)
Height (m)	1.7 (1.54–1.92)
BSA	1.92 (1.63–2.54)
SCR	0.90 (0.58–1.67)
Race	Caucasians—40
Gemcitabine doses ($mg\,m^{-2}$)	1000 (600–1500)
Rate of infusion ($mg\,m^{-2}\,min^{-1}$)	30.3 (8.11–49.52)
Chemotherapy	
Gemcitabine alone	32
Gemcitabine + carboplatin	2
Gemcitabine + bortezomib	6
Smoking history	
Non-smokers	12
Current smokers	2
Ex-smokers	25
Cancer type	
NSCLC	8
Breast	5
Ovarian	3
Pancreatic	8
Sarcomas	7
Others	9
Genetic covariates	**(Minor allele frequency)**
CDA (rs1048977; C>T)	0.29
SLC29A1 (rs747199; C>G)	0.25
NT5C2 (rs11598702; T>C)	0.35
NT5C3 (rs6946062; C>T)	0.45
SLC28A1 (rs11853372; G>T)	0.38
SLC28A3 (rs4877831; C>G)	0.24
SLC28A3 (rs7867504; T>C)	0.35

Abbreviations: BSA = body surface area; NSCLC = non-small cell lung cancer; SCR = serum creatinine.

Pharmacokinetic modelling. The population pharmacokinetic analysis of gemcitabine and its metabolites, dFdU and dFdCTP, was performed by means of nonlinear mixed-effects modelling using NONMEM VII (GloboMax LLC, Hanover, MD, USA) on a personal computer (Intel Pentium D processor, Hillsboro, OR, USA). The first-order conditional estimation with interaction method and ADVAN6 subroutine were used for the analysis. Model selection between competing nested models was performed by the likelihood ratio test as well as graphical goodness-of-fit diagnostics using R (version 2.9.0, Vienna, Austria). For structural model, a significance level of 0.05 was used to distinguish between competing nested models. Model selection between non-nested models was performed by Bayesian information criterion (BIC), which was calculated by equation (1).

$$\mathrm{BIC} = -2\mathrm{LL}p \times \mathrm{Ln}(n) \quad (1)$$

where -2LL is the -2 times log likelihood of the model or NONMEM's OFV, p is the number of parameters of the model and Ln(n) is the natural log of the number of observations in the data.

A sequential model building approach, using the individual pharmacokinetic parameters method was used to develop the pharmacokinetic models for gemcitabine and its metabolites (Zhang *et al*, 2003). Multicompartment models, parameterised in terms of clearances (CL and Q) and volumes of distribution (V) were tested for each of the analytes during structural model building. Figure 1 shows a schematic representation of the pharmacokinetic models for gemcitabine, dFdU and dFdCTP. Initially, plasma gemcitabine concentrations were analysed and pharmacokinetic parameters were obtained. In the next step, the model for dFdU plasma concentrations was developed. A mass-balance study reported that within 24 h of administration of gemcitabine, a median of 77% of the administered dose was excreted in the urine, only 5% of which was unchanged gemcitabine (Abbruzzese *et al*, 1991). Therefore, the fraction of gemcitabine converted to dFdU was assumed to be 0.73, which is 95% of 0.77. Finally, the model for dFdCTP concentrations was developed. The volume of dFdCTP compartment was fixed to 5 ml based on the cell volume of 2.5×10^{10} PBMCs in 5 l of blood (Wheater *et al*, 1979; Cheung *et al*, 1982; Alberts *et al*, 2008). Saturable and first-order rate of formation of dFdCTP were tested in model development. Saturable rate of formation of dFdCTP

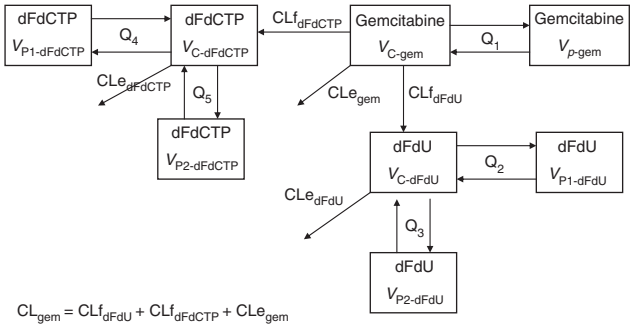

Figure 1. Pharmacokinetic model for gemcitabine, dFdU and dFdCTP. Q_1-Q_5 are inter-compartmental clearances; $V_{C\text{-}gem}$ and $V_{P\text{-}gem}$ are the volume of distribution of gemcitabine for central and peripheral compartment, respectively; CLf_{dFdU} and CLf_{dFdCTP} are the clearances associated with the formation of dFdU and dFdCTP, respectively; CLe_{gem} is the elimination clearance of gemcitabine by routes other than formation of dFdU and dFdCTP in PBMCs; CL_{gem} is the total elimination clearance of gemcitabine; $V_{C\text{-}dFdU}$, $V_{P1\text{-}dFdU}$ and $V_{P2\text{-}dFdU}$ are the volume of distribution of dFdU for central and peripheral compartments; CLe_{dFdU} is the elimination clearance of dFdU; $V_{C\text{-}dFdCTP}$, $V_{P1\text{-}dFdCTP}$ and $V_{P2\text{-}dFdCTP}$ are the volume of distribution of dFdCTP for central and peripheral compartments; CLe_{dFdCTP} is the elimination clearance of dFdCTP.

was described by the Michaelis–Menton model as shown in equation (2).

$$\text{Rate of dFdCTP formation} = \frac{V_{\max} \times C_{\text{gem}}}{EC_{50} \times C_{\text{gem}}} \quad (2)$$

where $V_{\max}$ is the maximum rate of dFdCTP formation; EC_{50} is the Michaelis–Menton constant in μM, which is the concentration of gemcitabine at which the rate of dFdCTP formation is half of $V_{\max}$; and C_{gem} is the gemcitabine plasma concentration in μM.

Forward inclusion and backward elimination strategy was used for covariate model building. A significance level of 0.01 was used for both forward inclusion and backward elimination steps. Table 1 shows the different covariates tested during the model building. Creatinine clearance (CL_{CR}) was estimated by the Cockcroft and Gault equation and BSA was calculated by the Du Bois and Du Bois formula (Cockcroft and Gault, 1976; Du Bois and Du Bois, 1989). Covariate model was built multiplicatively as shown in equation (3). Categorical covariates, for example, gender and genotype, were modelled using indicator variables. Continuous covariates were modelled by scaling the covariates by a clinically relevant value of the covariate as shown in equation (3) for BSA.

$$\text{TVP} = \theta_1 \times \left(\frac{\text{BSA}}{1.76}\right)^{\theta_2} \times \theta_3^{\text{IND}} \quad (3)$$

where IND is an indicator variable, which, for instance, for testing the effect of gender has a value of 1 for men and 0 for women, θ_1 is the typical value of the parameter (TVP) for female patients with BSA of 1.76 m^2, θ_3 is the fractional change in the TVP for male relative to female patients, θ_2 is the exponent of scaled BSA term in the model.

The inter-individual variability (IIV) on the PK parameters was modelled according to log-normal distribution as described by equation (4):

$$P_i = \text{TVP} \times \exp(\eta_i) \quad (4)$$

where P_i is the parameter estimate for the ith individual, TVP is the typical value of the parameter P and η_i is a random variable, which accounts for the inter-individual difference between P_i and TVP. The values of η_i were assumed to come from a normal distribution with mean of zero and variance ω^2.

The RUV in the concentrations was described by a proportional error model for gemcitabine and dFdU as described by equation (5) and combined error model for dFdCTP as described by equation (6) below.

$$C_{ij} = F_{ij} \times (1 + \varepsilon_{1ij}) \quad (5)$$

$$C_{ij} = F_{ij} \times (1 + \varepsilon_{1ij}) + \varepsilon_{2ij} \quad (6)$$

where C_{ij} and F_{ij} are the observed and predicted concentrations, respectively, in the ith individual at jth time point; ε_{1ij} and ε_{2ij} are the random residual deviations between the observed (C_{ij}) and predicted (F_{ij}) concentrations. The values of ε_{1ij} and ε_{2ij} were assumed to be independent from each other and come from a normal distribution with mean zero and variances σ_1^2 and σ_2^2, respectively. A separate RUV parameter (σ^2) was tested for the different assays used for the analysis of concentrations and included in the model if found significant at the α level of 0.05.

Model validation. The population pharmacokinetic model was evaluated by performing visual predictive checks and nonparametric bootstrap analysis. For the predictive check, 1000 data sets were simulated from each model using the final model parameters. The median, 5th and 95th percentiles of the simulated concentrations were calculated and compared with the observed data. Bootstrap analysis was done to assess the stability of pharmacokinetic models and to get the precision of the parameter estimates. For the bootstrap analysis, 1000 bootstrap runs were performed. In this technique, the final model developed from the original data set was fitted to each of the bootstrap data sets to obtain the bootstrap parameter estimates. The median, 2.5th and 97.5th percentiles of the parameter estimates were computed from the bootstrap runs and compared with the point estimates and 95% confidence intervals from the original data set.

RESULTS

Patients. A total of 335 gemcitabine concentrations, 454 dFdU concentrations and 373 dFdCTP concentrations from 40 patients who received gemcitabine as intravenous infusion were used in the model development. Patients received gemcitabine doses in the range of 600–1500 mg m^{-2}. Rate of infusion (ROI) of gemcitabine varied from 8.11 to 49.52 mg m^{-2} min^{-1}. Table 1 summarises the patient characteristics, dosing information and potential covariates used in the analysis. Thirty-two patients received gemcitabine as single-agent therapy, six patients received bortezomib 1 h after the end of gemcitabine infusion and two patients received carboplatin after gemcitabine infusion.

Pharmacokinetics of gemcitabine, dFdU and dFdCTP. Gemcitabine concentrations in the plasma samples collected after 6 h post infusion were below the LLOQ of the assay; however, dFdU and dFdCTP were measured up to 72 h post infusion. The pharmacokinetics of gemcitabine was best described by a two-compartment model. The parameter estimates of gemcitabine model are shown in Table 2. BSA and NT5C2 genotype were found to be significant covariates for elimination clearance, CL_{gem} of gemcitabine. CL_{gem} was estimated to be 425 l h^{-1} for a typical individual with a BSA of 1.76 m^2 and homozygous or heterozygous for the minor NT5C2 allele (CC or CT genotype). The covariate relationship of BSA and NT5C2 genotype with CL_{gem} has been described by equation (7), where NT5C2 = 1 for those homozygous for the major allele and 0 for presence of minor allele. An increase in BSA was associated with an increase in CL_{gem} and presence of homozygous major allele for NT5C2 (TT genotype) with an 18% decrease in CL_{gem}.

$$CL_{\text{gem}} = 425 \times \left(\frac{\text{BSA}}{1.76}\right) \times 0.816^{\text{NT5C2}} \quad (7)$$

BSA and age were found to be the significant covariates for volume of distribution of gemcitabine in the central compartment, $V_{C\text{-}gem}$. The estimate of $V_{C\text{-}gem}$ was 114 l for a typical individual with BSA of 1.76 m^2 and age of 70 years. The covariate relationship of BSA and age with $V_{C\text{-}gem}$ has been described by equation (8), which shows that an increase in BSA was associated with an increase in $V_{C\text{-}gem}$, while an increase in age was associated with a decrease in $V_{C\text{-}gem}$.

$$V_C\text{gem} = 114 \times \left(\frac{\text{BSA}}{1.76}\right) \times \left(\frac{\text{AGE}}{70}\right)^{-0.340} \quad (8)$$

The exponent of the effect of age on $V_{C\text{-}gem}$ was -0.340, which suggests increase in age is associated with decrease in the volume of distribution of gemcitabine. All of the parameters of gemcitabine pharmacokinetic model were precisely estimated, except the IIV of $V_{C\text{-}gem}$, which had a relative s.e. of 65.1%. The RUV in gemcitabine plasma concentration data was 24.9%. We tested the estimation of separate RUV parameters for the HPLC-UV and LC-MS/MS assays used in the analysis of gemcitabine plasma samples; however, only single RUV parameter explained the data best. The observed versus population-predicted gemcitabine concentration plot is shown in Figure 2A.

The concentration–time profiles of dFdU were best described by a three-compartment model. The parameter estimates of dFdU model are shown in Table 3. Creatinine clearance and CDA genotype were found to be significant covariates for CLe_{dFdU}, the elimination clearance of dFdU. CLe_{dFdU} was estimated to be 3.04 l h^{-1} for a typical individual with CL_{CR} of 75 ml min^{-1} and homozygous for the major CDA allele (CC genotype). BSA was found to be a significant covariate for the volume of distribution of dFdU for the central compartment, $V_{C\text{-}dFdU}$, which was estimated to be 16.1 l for a typical individual with BSA of 1.76 m^2.

Table 2. Parameter estimates for gemcitabine pharmacokinetic model

Parameter (unit)	Estimate (RSE%)	Bootstrap median (95% CI)
CL_{gem} (l h^{-1} 1.76 m^{-2})	425.0 (7.44)	419.3 (361.8, 485.8)
NT5C2 on CL_{gem}	0.816 (8.49)	0.823 (0.689, 0.938)
$V_{C\text{-}gem}$ (l 1.76 m^{-2} per 70 years)	114.0 (6.00)	114.8 (102.1, 127.3)
Exponent of AGE on $V_{C\text{-}gem}$	−0.340 (39.7)	−0.337 (−0.765, 0.07)
Q_1 (l h^{-1})	10.1 (28.6)	10.9 (6.2, 23.4)
$V_{P\text{-}gem}$ (l)	101.0 (50.5)	110.3 (39.5, 447.4)
IIV—CL_{gem}	22.2 (32.8)	21.3 (14.7, 29.7)
IIV—$V_{C\text{-}gem}$	12.9 (65.1)	11.5 (0.5, 21.5)
IIV—Q_1	97.6 (31.2)	92.6 (60.9, 124.3)
IIV—$V_{P\text{-}gem}$	87.5 (38.9)	61.6 (0.3, 114.5)
RUV (CV%)	24.9 (16.9)	24.9 (21.4, 28.9)

Abbreviations: CI = confidence interval; IIV = inter-individual variability, expressed as CV%; RSE = relative s.e., expressed as CV%; RUV = random unexplained variability, expressed as CV%.

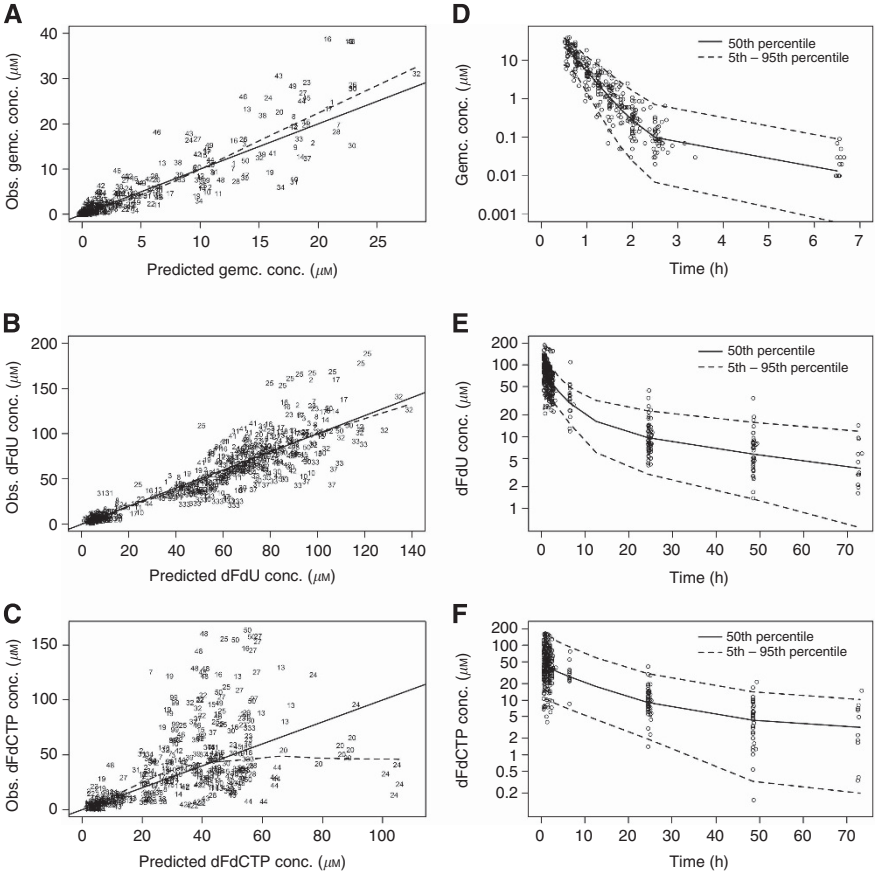

Figure 2. Observed (Obs.) versus population-predicted concentration plots for (A) gemcitabine, (B) dFdU and (C) dFdCTP based on the final model. Gemc = gemcitabine; dotted line in the plots represents lowess smooth through the data. Visual predictive check of the final population model for (**D**) gemcitabine, (**E**) dFdU and (**F**) dFdCTP. Observed data are represented by open circles. The simulated medians (50th percentile) are shown by the solid lines and the 90% prediction intervals by the dashed lines. Concentrations are in μM.

Table 3. Parameter estimates for dFdU pharmacokinetic model

Parameter (units)	Estimate (RSE%)	Bootstrap median (95% CI)
CLe_{dFdU} ($l\,h^{-1}$ per CL_{CR} 75 $ml\,min^{-1}$)	3.04 (11.2)	3.05 (2.42, 3.63)
CDA on CLe_{dFdU}	1.43 (13.2)	1.43 (1.14, 1.86)
$V_{C\text{-}dFdU}$ ($l\,1.76\,m^{-2}$)	16.1 (15.7)	16.1 (10.7, 21.9)
Q_2 ($l\,h^{-1}$)	70.4 (13.5)	70.7 (49.4, 90.6)
Q_3 ($l\,h^{-1}$)	32.6 (7.39)	32.9 (29.0, 37.8)
$V_{P1\text{-}dFdU}$ (l)	6.36 (8.77)	6.29 (5.27, 7.55)
$V_{P2\text{-}dFdU}$ (l)	113 (10.1)	112.8 (93.6, 135.6)
IIV—CLe_{dFdU}	41.2 (30.9)	40.3 (30.4, 53.3)
IIV—$V_{C\text{-}dFdU}$	62.9 (31.3)	61.7 (43.8, 83.4)
IIV—$V_{P1\text{-}dFdU}$	34.9 (27.4)	34.6 (25.6, 48.1)
IIV—$V_{P2\text{-}dFdU}$	54.6 (35.6)	52.2 (29, 69.0)
RUV	9.89 (32.8)	9.8 (7.5, 12.6)

Abbreviations: CI = confidence interval; IIV = inter-individual variability, expressed as CV%; RSE = relative s.e., expressed as CV%; RUV = random unexplained variability, expressed as CV%.

Table 4. Parameter estimates for dFdCTP pharmacokinetic model

Parameter	Estimate	Bootstrap median (95% CI)
CLf_{dFdCTP} ($l\,h^{-1}$) ROI < 25	0.118	0.128 (0.071, 0.235)
CLf_{dFdCTP} ($l\,h^{-1}$) ROI > 25	0.061	0.065 (0.041, 0.101)
SLC28A3 on CLf_{dFdCTP}	1.77	1.78 (1.10, 2.56)
CLe_{dFdCTP} ($l\,h^{-1}$)	0.00131	0.00152 (0.0007, 0.0023)
$V_{C\text{-}dFdCTP}$ (l)	0.005	—
Q_2 ($l\,h^{-1}$)	0.206	0.27 (0.077, 0.774)
Q_3 ($l\,h^{-1}$)	0.00126	0.0014 (0.0008, 0.0023)
$V_{P1\text{-}dFdCTP}$ (l)	0.0288	0.029 (0.017, 0.048)
$V_{P2\text{-}dFdCTP}$ (l)	0.0877	0.078 (0.017, 0.221)
IIV—CLf_{dFdCTP}	54.6	51.9 (37.2, 64.3)
IIV—$V_{P1\text{-}dFdCTP}$	36.9	38.7 (17.5, 59.8)
IIV—Q_2	186	194.2 (124.9, 270.4)
RUV-proportional (CV%)	32.2	31.9 (27.7, 35.4)
RUV-additive (s.d.)	1.33	1.33 (0.725, 1.39)

Abbreviations: CI = confidence interval; CV = coefficient of variation; IIV = inter-individual variability, expressed as CV%; ROI = rate of infusion of gemcitabine, expressed as $mg\,m^{-2}\,min^{-1}$; RUV = random unexplained variability, expressed as CV%; s.d. = standard deviation.

The covariate relationships of CL_{CR} and CDA genotype with CLe_{dFdU} were CDA = 1 for homozygous major allele and 0 for presence of minor allele (TT or CT genotype), and BSA with $V_{C\text{-}dFdU}$ are described as follows

$$CLe_{dFdU} = 3.04 \times \left(\frac{CL_{CR}}{75}\right) \times 1.43^{CDA} \quad (9)$$

$$V_C dFdU = 16.1 \times \left(\frac{BSA}{1.76}\right) \quad (10)$$

The parameters of dFdU model were estimated with good precision with relative s.e. in the range of 7–36%. The RUV in dFdU plasma concentration data was 9.89%. The observed versus population-predicted dFdU concentration plot is shown in Figure 2B.

The concentration–time profiles of dFdCTP were adequately described by a three-compartment model. The parameter estimates of dFdCTP model are shown in Table 4. The model with saturable formation of dFdCTP resulted in just three points drop in OFV as compared with the model with first-order formation. In model comparison, the model with saturable formation of dFdCTP had BIC slightly greater than the one with linear formation. Hence, the model with first-order formation of dFdCTP was selected for covariate model building and testing the effect of ROI of gemcitabine on the disposition parameters of dFdCTP. The formation clearance of dFdCTP, which is the part of the total plasma clearance of gemcitabine responsible for the formation of dFdCTP in PBMCs, CLf_{dFdCTP}, was found to be almost two-fold higher in the patients who received gemcitabine at a ROI $< 25\,mg\,m^{-2}\,min^{-1}$ ($0.118\,l\,h^{-1}$) than otherwise ($0.061\,l\,h^{-1}$). The cutoff value of $25\,mg\,m^{-2}\,min^{-1}$ was chosen based on the maximum drop in NONMEM OFV. Several different cutoff values of ROI were tested in the model development, but $25\,mg\,m^{-2}\,min^{-1}$ was found to be associated with maximum decrease in the NONMEM OFV, which was significant at α level of 0.01. Presence of homozygous major allele for SLC28A3 (CC genotype) was associated with an almost two-fold increase (1.77) in the formation clearance of dFdCTP. The RUV was estimated to be 32.2% from the proportional component and the s.d. of the additive component was 1.33 μM. The observed versus population-predicted dFdCTP concentration plot is shown in Figure 2C.

Other goodness-of-fit plots, such as conditional-weighted residuals versus time and population prediction were also evaluated during the model development for gemcitabine, dFdU and dFdCTP. None of these plots showed any evidence of model misspecification (data not shown).

As mentioned previously, only eight patients received combination chemotherapy, in which six patients received bortezomib 1 h after the end of gemcitabine infusion and two patients received carboplatin immediately after the end of gemcitabine infusion. In the course of model development, we tested whether co-administration of bortezomib affects the disposition of gemcitabine and/or its metabolites. Bortezomib co-administration was not found to affect the disposition of gemcitabine and its metabolites. Effect of carboplatin co-administration was not tested in the model development because of the limited sample size of only two patients.

Model validation. The predictive check plots of gemcitabine and its metabolites are depicted in Figure 2D–F. The predictive check plots show that the model has adequately described the overall trend and variability in the observed data. No systematic deviation was observed between the observed and simulated data. The percentage of observations outside the 90% confidence interval for gemcitabine, dFdU and dFdCTP were 7.76, 10.6 and 5.09%.

In the bootstrap analysis, 86%, 96.2% and 90.5% of gemcitabine, dFdU and dFdCTP runs, respectively, were minimised successfully. The median of bootstrap parameter estimates were similar to the NONMEM estimates based on original data set.

DISCUSSION

The majority of the patients in this study received gemcitabine as a single agent, and six subjects also received bortezomib (not a significant covariate in the model) and two received carboplatin. This is the first prospective study to develop a population

pharmacokinetic model for gemcitabine and metabolites that accounts at least partly for the long half-life for the active metabolite, dFdCTP. Previous investigators have evaluated dFdCTP disposition up to 2 h after the end of gemcitabine infusion (Tempero *et al*, 2003; Tham *et al*, 2008; Joerger *et al*, 2012); however, sampling PBMCs over a longer period would be more informative to provide a better understanding of the disposition of dFdCTP and determination of the effect of patient-specific covariates on pharmacokinetics of dFdCTP. The PBMC dFdCTP concentrations were measured over 72 h samples post infusion, which spanned over three half-lives. Covariates associated with drug and metabolite pharmacokinetic variability were assessed including patient demographics (for example, BSA and age), renal function estimates and genotypes in gemcitabine metabolic pathway genes. As NONMEM does not enable rapid analyses of the >110 SNPs that we initially identified within the gemcitabine metabolic pathway, a previous analysis was used to guide selection of the seven SNPs that would be tested as part of the final model reported in this paper (Mitra *et al*, 2012).

Our estimates for gemcitabine and dFdU pharmacokinetic parameters (that is, clearance and volume of distribution) closely approximate the estimates reported by others (Grunewald *et al*, 1992; Venook *et al*, 2000; Soo *et al*, 2003). Both elimination clearance and volume of distribution of gemcitabine were dependent on BSA, which is consistent with the clinical practice of BSA-based dosing. The NT5C2 promoter SNP (rs11598702; T>C) has been previously associated with expression levels for this enzyme, and we observed an effect on gemcitabine clearance from plasma (higher). This SNP occurs in LD with two other SNPs (rs1163238 and rs11191612) located in the promoter region of the gene. NT5C2 dephosphorylates monophosphorylated gemcitabine, so in theory, genetic variants in this enzyme would be expected to affect the intracellular balance of the parent drug and dFdCTP. It is not clear how this affects the clearance from plasma, and studies that measure gemcitabine concentrations in PBMC's (in addition to dFdCTP) would provide insight on this observation (Bapiro *et al*, 2011). Increase in age was found to be associated with decrease in volume of distribution of gemcitabine. With aging, the body's fat composition increases while the water composition decreases. Gemcitabine being a hydrophilic drug could have lower volume of distribution because of decrease in water composition with aging. Plasma and liver CDA-based metabolism of gemcitabine to dFdU is the major pathway for gemcitabine elimination. We did not observe an effect of the CDA synonymous SNP (rs1048977; C>T) on gemcitabine clearance; however, there was association with reduced dFdU clearance. As there were only three subjects who were homozygous for this variant, we included those who were heterozygous, although their estimated dFdU clearance more closely approximated that of the homozygous common allele. It remained statistically significant in the model, however, and further evaluation in larger studies are warranted to rule out the statistical significance of CDA (rs1048977; C>T) to be observed due to type-I error. We and others have demonstrated that dFdU contributes towards antitumour effect and toxicity, most probably through the formation of phosphorylated metabolites of intracellular dFdU (Pauwels *et al*, 2006; Veltkamp *et al*, 2008; Benyumov *et al*, 2011). As shown by others, we also found CL_{CR} to be a significant predictor for the elimination clearance of dFdU, which is not surprising as dFdU is primarily excreted by the kidneys (Jiang *et al*, 2008). BSA was found to be a predictor for the volume of distribution of dFdU, which is consistent with another report (Jiang *et al*, 2008).

Previously, dFdCTP pharmacokinetics has been described by a one-compartment model (Tham *et al*, 2008; Joerger *et al*, 2012); however, we found that it was best described by a three-compartment model. As mentioned above, this discrepancy is probably attributable to the longer sampling scheme that we used. Tham *et al* (2008) reported that linear formation of dFdCTP best describes dFdCTP formation at clinically used doses of gemcitabine. In the present study, the model with saturable formation of dFdCTP had three points lower OFV than the model with linear formation, which indicated a weak signal for saturable formation of dFdCTP, which could be due to small sample size in the current study. The estimate of EC_{50} was 8.7 μM, which is comparable to the 10–20 μM concentration range *in vitro* at which the formation of dFdCTP becomes saturated (Grunewald *et al*, 1990; Grunewald *et al*, 1991). The two models, one with saturable formation of dFdCTP and the other with linear formation, being non-nested models were compared with BIC. After model comparison, the model with linear formation of dFdCTP was selected over the model with saturable formation because of its lower BIC. As the data provided a weak signal for saturable formation of dFdCTP, which was not significant, we tested the effect of ROI of gemcitabine on the formation of dFdCTP. The ROI of gemcitabine was found to be a significant covariate for the formation of dFdCTP. The ROI of gemcitabine in the study ranged from 8.11 to 49.52 $mg\,m^{-2}\,min^{-1}$. The effect of ROI of gemcitabine on formation of dFdCTP was modelled as a dichotomous variable because of the limited sample size in the study. The dependence of formation of dFdCTP on ROI of gemcitabine indicates saturable formation of this metabolite and is consistent with the *in vitro* literature (Grunewald *et al*, 1990, 1991).

The comparison of fixed dose rate (FDR) infusion (10 $mg\,m^{-2}\,min^{-1}$) with standard ROI (1000 $mg\,m^{-2}$ over 30 min, 33.3 $mg\,m^{-2}\,min^{-1}$) of gemcitabine for clinical effectiveness has also shown conflicting results. Some studies showed that FDR is superior to the standard infusion (Ceribelli *et al*, 2003; Tempero *et al*, 2003). Others have shown no improvement in the efficacy with FDR as compared with the standard infusion; unfortunately, these studies did not involve pharmacokinetic study of dFdCTP, which could have explained whether the lack of superiority of FDR infusion is due to linear pharmacokinetics of dFdCTP (Cappuzzo *et al*, 2006; Soo *et al*, 2006). Several authors have shown higher rate of dFdCTP formation at FDR compared with the standard ROI of gemcitabine (Patel *et al*, 2001; Tempero *et al*, 2003; Grimison *et al*, 2007). Our results appear to be consistent with others, as we also observed higher formation of dFdCTP at lower ROI ($ROI < 25\ mg\,m^{-2}\,min^{-1}$) as compared with $ROI > 25\ mg\,m^{-2}\,min^{-1}$. However, owing to small sample size, we could not test whether the formation of dFdCTP could be even higher at FDR infusion.

Although infusion rate was associated with higher formation clearance of dFdCTP in our studies, there is high between-patient variability in the concentrations measured. For example, Tempero *et al* (2003) evaluated concentrations in patients who all received similar doses, and the data show up to a 2 log-fold range in concentrations. Gemcitabine is transported into cells via members of the nucleoside transporter family. Two equilibrative nucleoside transporters, SLC29A1 and SLC29A2, and three concentrative nucleoside transporters, SLC28A1, SLC28A2 and SLC28A3 are involved in the intracellular transport, with SLC29A1, SLC28A1 and SLC28A3 being the primary mediators (Ueno *et al*, 2007; Wong *et al*, 2009). Saturation of these transporters at higher infusion rate could result in the decrease in formation of intracellular dFdCTP. Presence of genetic variants for these transporters could contribute to the dFdCTP variability that we and others have observed. Our results indicate an association between a synonymous SNP in the coding region of SCL28A3 (rs7867504; T>C) and decreased dFdCTP formation clearance. It is provocative to ask whether patients with genetic variation in key transporter/metabolic pathway proteins such as this might be good candidates to receive FDR infusion gemcitabine, relative to those with common alleles. Metharom *et al* (2011) demonstrated the advantage of FDR infusion for subjects with variant alleles in

CDA in one small study. Hence, there may be a greater advantage to administering FDR gemcitabine to selected patients as opposed to an unselected population.

This was an open enrollment study protocol in which the majority of the patients had prior treatment with chemotherapy, including gemcitabine, before being enrolled in the study. Our study was not designed to collect detailed information about adverse effects following gemcitabine administration; however, we collected information about complete blood count before the administration of gemcitabine on the day of the study and again at the time of next gemcitabine dose in the treatment cycle. As the time interval between the two visits, before and after gemcitabine administration, ranged from 1 to 2 weeks, the blood cell counts were already recovered to the pretreatment levels in all of the patients. This could be one of the limitations of our study as it was not possible to study the exposure–toxicity relationship under this design. Another limitation of this study is the small sample size of 40 patients of which there were very limited number of patients who received gemcitabine at slower ROI and presence of genetic variants. For example, two variant alleles affecting CDA activity the rs2072671 79A>C SNP and promoter SNP rs532545 that occurs in LD (D′0.92) with del31C were both genotyped in this study. The 79 A>C SNP is a culprit for decreased CDA activity (Tibaldi *et al*, 2008) and del31C associated with ultra-metaboliser phenotype (Caronia *et al*, 2011) and capecitabine metabolism. However, these SNPs were not associated with PK parameters and may be due to small sample size, as only three subjects with homozygous variant genotype for these two SNPs were observed.

In conclusion, BSA and age were found to be the important covariates for the disposition of gemcitabine; BSA and CL_{CR} were found to be the important covariates for dFdU; and ROI was found to be an important covariate for the formation clearance of dFdCTP. We found that patients who received gemcitabine at a ROI $< 25\ mg\ m^{-2}\ min^{-1}$ have higher formation clearance than those who received it at ROI $> 25\ mg\ m^{-2}\ min^{-1}$. Hence, administration of gemcitabine at a lower ROI $< 25\ mg\ m^{-2}\ min^{-1}$ is expected to result in greater exposure of dFdCTP. Dependence of elimination clearance and volume of distribution on BSA was in agreement with the BSA-based dosing of gemcitabine. Three genetic variants were also significant in the model, and larger studies in a more focused population (that is, same disease state, first chemotherapy and so on) would enable better determination of the importance of these and others on patient toxicity. The final model was judged adequate by bootstrap analysis and visual predictive check.

ACKNOWLEDGEMENTS

This study was sponsored by a Clinical Scholars Award to MNK, and R01CA132946 to JKL. Analyses of gemcitabine, dFdU and dFdCTP concentrations were conducted by the Clinical Pharmacology Shared Resource, which is supported in part by Cancer Center Support (MN, USA) Grant (5P30 CA77598). We thank the study patient volunteers who donated their valuable time towards the goals of the project. We also thank Linda Kruse, study coordinator, for her outstanding contribution of enrolling the study volunteers and supervising blood sample collection.

REFERENCES

Abbruzzese JL, Grunewald R, Weeks EA, Gravel D, Nowak B, Mineishi S, Tarassoff P, Satterlee W, Raber MN (1991) A phase I clinical, plasma, and cellular pharmacology study of gemcitabine. *J Clin Oncol* **9**(3): 491–498.

Alberts B, Johnson A, Lewis J, Raff M, Roberts K, Walter P (2008) *Molecular Biology of the Cell*. Garland Science: NY, USA.

Bapiro TE, Richards FM, Goldgraben MA, Olive KP, Madhu B, Frese KK, Cook N, Jacobetz MA, Smith DM, Tuveson DA, Griffiths JR, Jodrell DI (2011) A novel method for quantification of gemcitabine and its metabolites 2',2'-difluorodeoxyuridine and gemcitabine triphosphate in tumour tissue by LC-MS/MS: comparison with (19)F NMR spectroscopy. *Cancer Chemother Pharmacol* **68**(5): 1243–1253.

Benyumov A, Gurvich VJ, Lis LG, Williams BW, Kirstein MN (2011) Combinatorial pharmacologic effects of gemcitabine and its metabolite dFdU. *Chem Med Chem* **6**(3): 457–464.

Bogachev VS (1996) Synthesis of deoxynucleoside 5'-triphosphates using trifluoroacetic anhydride as an activating reagent. *Bioorganicheskaya Khimiya* **22**: 699–705.

Cappuzzo F, Novello S, De Marinis F, Selvaggi G, Scagliottl GV, Barbieri F, Maur M, Papi M, Pasquini E, Bartolini S, Marini L, Crinò L (2006) A randomized phase II trial evaluating standard (50 mg/min) versus low (10 mg/min) infusion duration of gemcitabine as first-line treatment in advanced non-small-cell lung cancer patients who are not eligible for platinum-based chemotherapy. *Lung Cancer* **52**(3): 319–325.

Caronia D, Martin M, Sastre J, de la Torre J, Garciá-Sáenz JA, Alonso MR, Moreno LT, Pita G, Díaz-Rubio E, Benítez J, González-Neira A (2011) A polymorphism in the cytidine deaminase promoter predicts severe capecitabine-induced hand-foot syndrome. *Clin Cancer Res* **17**(7): 2006–2013.

Ceribelli A, Gridelli C, De Marinis F, Fabi A, Gamucci T, Cortesi E, Barduagni M, Antimi M, Maione P, Migliorino MR, Giannarelli Cognetti F (2003) Prolonged gemcitabine infusion in advanced non-small cell lung carcinoma: a randomized phase II study of two different schedules in combination with cisplatin. *Cancer* **98**(2): 337–343.

Cheung RK, Grinstein S, Gelfand EW (1982) Volume regulation by human lymphocytes. Identification of differences between the two major lymphocyte subpopulations. *J Clin Invest* **70**(3): 632–638.

Cockcroft DW, Gault MH (1976) Prediction of creatinine clearance from serum creatinine. *Nephron* **16**(1): 31–41.

Du Bois D, Du Bois EF (1989) A formula to estimate the approximate surface area if height and weight be known. 1916. *Nutrition* **5**(5): 303–311 (discussion 312–303).

Grimison P, Galettis P, Manners S, Jelinek M, Metharom E, de Souza PL, Liauw W, Links MJ (2007) Randomized crossover study evaluating the effect of gemcitabine infusion dose rate: evidence of auto-induction of gemcitabine accumulation. *J Clin Oncol* **25**(36): 5704–5709.

Grunewald R, Abbruzzese JL, Tarassoff P, Plunkett W (1991) Saturation of 2',2'-difluorodeoxycytidine 5'-triphosphate accumulation by mononuclear cells during a phase I trial of gemcitabine. *Cancer Chemother Pharmacol* **27**(4): 258–262.

Grunewald R, Kantarjian H, Du M, Faucher K, Tarassoff P, Plunkett W (1992) Gemcitabine in leukemia: a phase I clinical, plasma, and cellular pharmacology study. *J Clin Oncol* **10**(3): 406–413.

Grunewald R, Kantarjian H, Keating MJ, Abbruzzese J, Tarassoff P, Plunkett W (1990) Pharmacologically directed design of the dose rate and schedule of 2',2'-difluorodeoxycytidine (Gemcitabine) administration in leukemia. *Cancer Res* **50**(21): 6823–6826.

Jiang X, Galettis P, Links M, Mitchell PL, McLachlan AJ (2008) Population pharmacokinetics of gemcitabine and its metabolite in patients with cancer: effect of oxaliplatin and infusion rate. *Br J Clin Pharmacol* **65**(3): 326–333.

Joerger M, Burgers JA, Baas P, Doodeman VD, Smits PH, Jansen RS, Vainchtein LD, Rosing H, Huitema AD, Beijnen JH, Schellens JH (2012) Gene polymorphisms, pharmacokinetics, and hematological toxicity in advanced non-small-cell lung cancer patients receiving cisplatin/gemcitabine. *Cancer Chemother Pharmacol* **69**(1): 25–33.

Kirstein MN, Hassan I, Guire DE, Weller DR, Daqit JW, Fisher JE, Remmel RP (2006) High-performance liquid chromatographic method for the determination of gemcitabine and 2',2'-difluorodeoxyuridine in plasma and tissue culture media. *J Chromatogr B Analyt Technol Biomed Life Sci* **835**(1-2): 136–142.

Lohman GJS, Stubbe J (2010) Inactivation of Lactobacillus leichmannii ribonucleotide reductase by 2 ',2 '-difluoro-2 '-deoxycytidine 5 '-triphosphate: covalent modification. *Biochemistry* **49**(7): 1404–1417.

Metharom E, Galettis P, Manners S, Jelinek M, Liauw W, de Souza PL, Hoskins JM, Links M (2011) The pharmacological advantage of prolonged dose rate gemcitabine is restricted to patients with variant alleles of cytidine deaminase c.79A>C. *Asia-Pacific J Clin Oncol* **7**(1): 65–74.

Mitra AK, Kirstein MN, Khatri A, Skubitz KM, Dudek AZ, Greeno EW, Kratzke RA, Lamba JK (2012) Pathway-based pharmacogenomics of gemcitabine pharmacokinetics in patients with solid tumors. *Pharmacogenomics* **13**(9): 1009–1021.

Patel SR, Gandhi V, Jenkins J, Papadopolous N, Burgess MA, Plager C, Plunkett W, Benjamin RS (2001) Phase II clinical investigation of gemcitabine in advanced soft tissue sarcomas and window evaluation of dose rate on gemcitabine triphosphate accumulation. *J Clin Oncol* **19**(15): 3483–3489.

Pauwels B, Korst AE, Lambrechts HA, Pattyn GG, de Pooter CM, Lardon F, Vermorken JB (2006) The radiosensitising effect of difluorodeoxyuridine, a metabolite of gemcitabine, in vitro. *Cancer Chemother Pharmacol* **58**(2): 219–228.

Risbood PA, Kane Jr CT, Hossain MT, Vadapalli S, Chadda SK (2008) Synthesis of gemcitabine triphosphate (dFdCTP) as a tris(triethylammonium) salt. *Bioorg Med Chem Lett* **18**(9): 2957–2958.

Soo RA, Lim HL, Wang LZ, Lee HS, Millward MJ, Tok LT, Lee SC, Lehnert M, Goh BC (2003) Phase I trial of fixed dose-rate gemcitabine in combination with carboplatin in chemonaive advanced non-small-cell lung cancer: a Cancer Therapeutics Research Group study. *Cancer Chemother Pharmacol* **52**(2): 153–158.

Soo RA, Wang LZ, Tham LS, Yong WP, Boyer M, Lim HL, Lee HS, Millward M, Liang S, Beale P, Lee SC, Goh BC (2006) A multicentre randomised phase II study of carboplatin in combination with gemcitabine at standard rate or fixed dose rate infusion in patients with advanced stage non-small-cell lung cancer. *Ann Oncol* **17**(7): 1128–1133.

Tempero M, Plunkett W, Ruiz Van Haperen V, Hainsworth J, Hochster H, Lenzi R, Abbruzzese J (2003) Randomized phase II comparison of dose-intense gemcitabine: thirty-minute infusion and fixed dose rate infusion in patients with pancreatic adenocarcinoma. *J Clin Oncol* **21**(18): 3402–3408.

Tham L-S, Wang L-Z, Soo RA, Lee HS, Lee SC, Goh BC, Holford NH (2008) Does saturable formation of gemcitabine triphosphate occur in patients? *Cancer Chemother Pharmacol* **63**(1): 55–64.

Tibaldi C, Giovannetti E, Vasile E, Mey V, Laan AC, Nannizzi S, Di Marsico R, Antonuzzo A, Orlandini C, Ricciardi S, Del Tacca M, Peters GJ, Falcone A, Danesi R (2008) Correlation of CDA, ERCC1, and XPD polymorphisms with response and survival in gemcitabine/cisplatin-treated advanced non-small cell lung cancer patients. *Clin Cancer Res* **14**(6): 1797–1803.

Ueno H, Kiyosawa K, Kaniwa N (2007) Pharmacogenomics of gemcitabine: can genetic studies lead to tailor-made therapy? *Br J Cancer* **97**(2): 145–151.

Veltkamp SA, Hillebrand MJX, Rosing H, Jansen RS, Wickremsinhe ER, Perkins EJ, Schellens JH, Beijnen JH (2006) Quantitative analysis of gemcitabine triphosphate in human peripheral blood mononuclear cells using weak anion-exchange liquid chromatography coupled with tandem mass spectrometry. *J Mass Spectrom* **41**(12): 1633–1642.

Veltkamp SA, Pluim D, van Eijndhoven MA, Bolijn MN, Ong FH, Govindarajan R, Unadkat JD, Beijnen JH, Schellens JH (2008) New insights into the pharmacology and cytotoxicity of gemcitabine and 2',2'-difluorodeoxyuridine. *Mol Cancer Ther* **7**(8): 2415–2425.

Venook AP, Egorin MJ, Rosner GL, Hollis D, Mani S, Hawkins M, Byrd J, Hohl R, Budman D, Meropol NJ, Ratain MJ (2000) Phase I and pharmacokinetic trial of gemcitabine in patients with hepatic or renal dysfunction: Cancer and Leukemia Group B 9565. *J Clin Oncol* **18**(14): 2780–2787.

Wheater PR, Burkitt HG, Daniels VG, Deakin PJ (1979) *Functional Histology: A Text And Color Atlas.* Churchill Livingstone: NY, USA.

Wong A, Soo RA, Yong W-P, Innocenti F (2009) Clinical pharmacology and pharmacogenetics of gemcitabine. *Drug Metab Rev* **41**(2): 77–88.

Zhang L, Beal SL, Sheiner LB (2003) Simultaneous vs. sequential analysis for population PK/PD data I: best-case performance. *J Pharmacokinet Pharmacodyn* **30**(6): 387–404.